Available online at www.sciencedirect.com
SCIENCE DIRECT®
Solar Energy 79 (2005) 495–504
SOLAR ENERGY
www.elsevier.com/locate/solener

Analysis of short-term solar radiation data

Gayathri Vijayakumar, Michaël Kummert, Sanford A. Klein *, William A. Beckman

Solar Energy Laboratory, University of Wisconsin, 1500 Engineering Drive, Madison, WI 53706, USA

Received 28 May 2004; received in revised form 18 November 2004; accepted 15 December 2004
Available online 25 February 2005

Communicated by: Associate Editor David Renne

Abstract

Solar radiation data are available for many locations on an hourly basis. Simulation studies of solar energy systems have generally used these hourly values to estimate long-term annual performance, although solar radiation can exhibit wide variations during an hour. Variations in solar radiation *during* an hour, such as on a minute basis, could result in inaccurate performance estimates for systems that respond quickly and non-linearly to solar radiation. In addition, diffuse fraction regressions and cumulative frequency distribution curves have been developed using hourly data and the accuracy of these regressions when applied to short-term radiation has not been established. The purpose of this research is to investigate the inaccuracies caused by using hourly rather than short-term (i.e., minute and 3 min) radiation data on the estimated performance of solar energy systems. The inaccuracies are determined by examination of the frequency distribution and diffuse fraction relationships for short-term solar radiation data as compared to existing regressions and by comparing calculated radiation on tilted surfaces and utilizability based on hourly and short-term radiation data.

Keywords: Solar radiation; Short-term; Minute; Tilted; Diffuse

1. Introduction

Analyses to predict long-term performances of solar energy systems rely on the availability of solar radiation data. These data generally include measurements of global horizontal radiation, diffuse radiation, and direct (beam normal) radiation. Hourly data are most commonly used in these analyses and are readily available. For example, hourly data for 239 US locations for 30 years are available through the National Solar Radiation Data Base (NSRDB, 1992), although much of the data in this database is based on estimated rather than measured information. Although solar radiation can vary significantly on times scales less than one hour, there are little available data for short time periods. Analyses of short-term radiation data have been published by Smietana et al. (1984), Saluja and Muneer (1986), Suehrcke and McCormick (1988), Skartveit and Olseth (1992) and Gansler (1993, 1995).

Fig. 1 provides a plot of solar radiation measured at 1-min intervals for one partially cloudy day. Also shown

* Corresponding author. Tel.: +1 608 263 5626; fax: +1 608 262 8469.
E-mail address: klein@engr.wisc.edu (S.A. Klein).

0038-092X/$ - see front matter © 2005 Elsevier Ltd. All rights reserved.
doi:10.1016/j.solener.2004.12.005

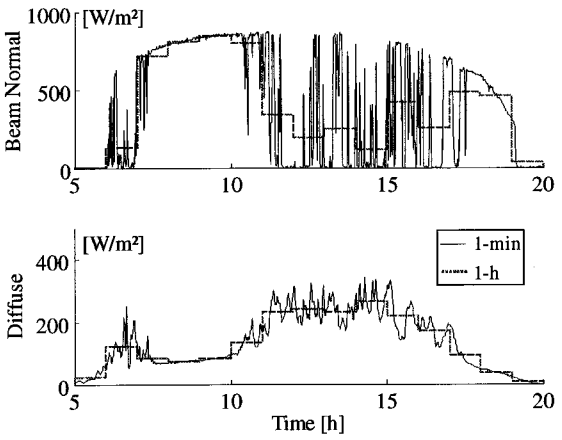

Fig. 1. 1-min versus hourly Beam normal and diffuse horizontal radiation for July 5 in Madison, WI.

in this figure is the corresponding hourly radiation that would normally be input to simulation programs. A comparison of the two short-term and hourly curves illustrates the information that is lost by using hourly data rather than minute data. This paper investigates how important that information is in analyses of solar energy conversion systems.

The data used in this paper were obtained from the Integrated Surface Irradiance Study network (ISIS, 2004), which is operated by the Surface Radiation Research Branch of the National Oceanic and Atmospheric Administration (NOAA/SRBB). The ISIS network provides measurements of solar radiation data on a 3-min basis for Albuquerque, NM, Bismarck, ND, Hanford, CA, Madison, WI, Oak Ridge, TN, Seattle, WA, Salt Lake City, UT, and Sterling, VA. Furthermore, 1-min data are also available for Madison, WI and Sterling, VA. In this study, 12 months were selected in the available data (January 2002–October 2004) for each location. The months were selected to avoid missing or bad data and to minimize the difference between the monthly average values (beam and global radiation) and the long-term averages. A description of the instruments used to measure solar radiation and the uncertainties associated with the measured data is provided on the ISIS website (ISIS, 2004) and in Table 1.

One- and three-minute radiation data were analyzed to determine diffuse fraction as a function of clearness index and to determine frequency distributions. The influence of air mass on these relationships was also investigated. The concept of solar radiation utilizability was used to assess the data in performance analyses of solar energy systems. Utilizability analyses are general, system-independent, and can be easily used to quantify the maximum differences in system performance resulting from using short-term and hourly solar radiation data, without the need to do specific system simulations (Klein and Beckman, 1984).

2. Data analysis

Short-term variations in solar radiation data have not been extensively investigated. In many cases, diffuse radiation data are not available and they must be estimated knowing only the total radiation. Previous studies of monthly-average, daily, hourly and to a lesser extent, minute data have shown that the diffuse fraction depends on the clearness index, defined as the ratio of the measured horizontal radiation to the horizontal extraterrestrial radiation for the same time period. The regression equation for daily diffuse fraction to daily clearness index is generally different from that for hourly diffuse radiation, as shown in Duffie and Beckman (1991). It is not known to what extent diffuse fraction regressions developed for hourly time intervals are applicable on shorter time scales. In addition, the variability of short-term radiation data and its effect on solar system performance have not been thoroughly investigated. One way to demonstrate the variability in short-term solar radiation data is through frequency distributions as has been done by Suehrcke and McCormick (1988) and Gansler et al. (1995). The distributions, and the solar radiation utilizability that depends on them, are investigated in this study.

2.1. Diffuse fraction

Solar energy systems generally utilize beam and diffuse radiation differently, so it is necessary to know the individual contributions in addition to their total. The

Table 1
Instruments used in the ISIS data network

Irradiance component	Instrument	Waveband (nm)	Mounting arrangement
Global horizontal	Black Surface Detector Precision Spectral Pyranometer (PSP)	280–3000	Unshaded, ventilated
Diffuse horizontal	Black and White Detector Pyranometer (B&WD)	280–3000	Shaded by ball or disc mounted on sun tracker, ventilated
Direct beam normal	Normal Incidence Pyrheliometer (NIP)	280–3000	Mounted on sun tracker

All instruments are re-calibrated on a yearly basis at the National Renewable Energy Laboratory.

estimation of radiation on a tilted surface also requires knowledge of the beam and diffuse components. If only total radiation is known, the diffuse and beam components can be estimated using diffuse fraction regressions.

Fig. 2 is a plot of the measured diffuse fraction as a function of clearness index based on 3-min data in Madison, WI for December 2002. (Note that data points very close to sunrise/set have been removed when the measured diffuse radiation is lower than 15 W/m^2.) This plot is typical of the diffuse fraction plots observed for other months and locations. In Fig. 2(a), the diffuse fractions were determined by dividing the measured diffuse horizontal irradiance by the measured global horizontal irradiance. This method is denoted "G, Gd" in the following discussion. Values larger than 1 are mainly caused by an erroneous offset that affects Solid Black Detector Precision Spectral Pyranometers (PSP), which are used to measure global radiation in the ISIS network. The offset can be attributed to infrared cooling of the glass hemispheres, which in turn cools the detector and causes a negative offset in the response produced by this instrument (Gulbrandsen, 1978). Correction methods have been developed for diffuse radiation measurements (Dutton et al., 2001) but they are not directly applicable to global radiation measurements. PSP's measuring global radiation are also affected by errors in the directional response, which can also lead to underestimated measurements.

Fig. 2(b) shows data for the same month as Fig. 2(a) using diffuse fractions calculated with the measured diffuse horizontal radiation and the measured beam normal radiation. This procedure is recommended by the World Climate Research Program's Baseline Surface Radiation Network (McArthur, 1998; cited in Dutton et al., 2001). It is denoted "Gbn, Gd" in the following discussion. The global horizontal radiation is determined by summing the calculated beam radiation on the horizontal surface (which is the product of the beam normal radiation and the cosine of the zenith angle) and the measured diffuse radiation. Diffuse fractions calculated in this manner are always between 0 and 1.

A third method of determining the diffuse irradiance from the available data is to use the measured direct beam normal to calculate the beam radiation on a horizontal surface and subtract the beam component from the measured horizontal irradiance. The effect of using diffuse radiation in these three ways on the calculated radiation for tilted surfaces is presented in the next section.

Fig. 2 also shows the diffuse fraction regression proposed by Erbs et al. (1982) based on hourly radiation measurements. Other diffuse fraction regressions are available, e.g., Reindl et al. (1990), Perez et al. (1988, 1992). However, Fig. 2 shows that any diffuse fraction model that is based solely on the clearness index will be subject to a significant scatter as other variables affect the short-term diffuse fraction. The scatter in the diffuse fraction regression equation becomes smaller for longer time periods, as noted by Saluja and Muneer (1986).

Fig. 3 shows the relationship of diffuse fraction to clearness index using for a single clear day in April in Oak Ridge, representative of clear days in other locations. The diffuse fraction regression developed by Erbs et al. (1982) is also shown. Fig. 3 indicates that, for a clear day, the diffuse radiation is overestimated when applying Erbs' regression for hourly data to the 3-min data. Note that all of the data points in Fig. 3 correspond to clear sky conditions. The variation in clearness index in this case is due to the change in air mass with time of day. This same behavior was observed for 1-min clear sky data in Madison, WI.

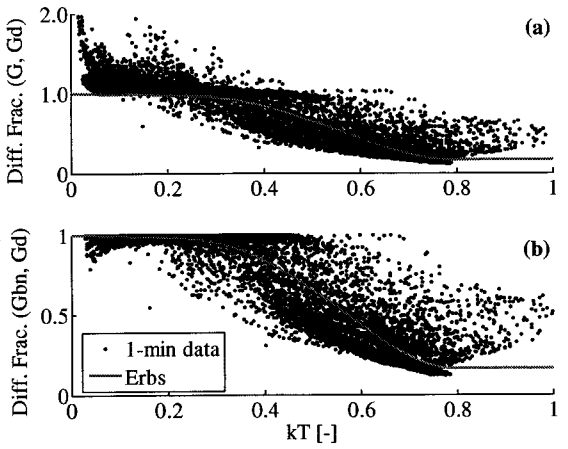

Fig. 2. 1-min Diffuse fraction as a function of clearness index for December 2002, in Madison, WI.

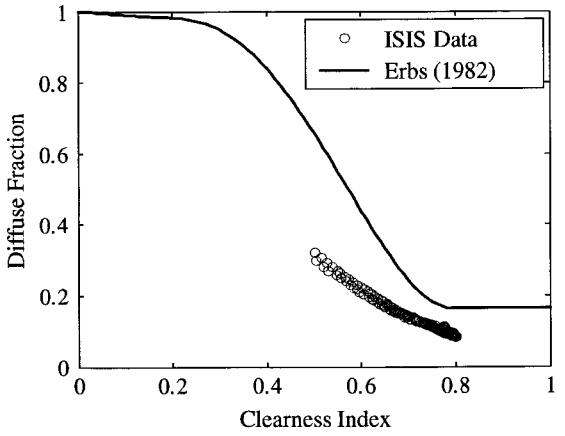

Fig. 3. Diffuse fraction as a function of clearness index for a clear April day in Oak Ridge, TN.

Gansler (1993) suggested that the diffuse fraction depends on other factors such as relative humidity, ambient temperature, and air mass. Air mass, m, is approximated here as

$$m = \frac{1}{\cos\theta_z} \tag{1}$$

where θ_z is the solar zenith angle. Fig. 4 shows the air mass dependence of diffuse fraction for 3-min radiation data for June 2002 in Hanford, CA. The dependence on air mass is apparent on clear days, and less so on cloudy and partly cloudy days.

Another way to demonstrate the influence of air mass on diffuse fraction for clear days is shown in Fig. 5. Fig. 5 shows diffuse fraction as a function of air mass for one clear winter day and one clear summer day, for Albuquerque, Seattle, and Madison. These stations were selected for their different climate types. It appears that the diffuse fraction is affected by the moisture content of the air as well as the ambient temperature as suggested by Iqbal (1983), Reindl et al. (1990) and Gansler (1993). Drier climates and cold winter months that have lower humidity values exhibit lower diffuse fractions than wetter climates and warmer months, due to increased scattering from water molecules in the air. The observed variations in diffuse fraction are much larger than what can be explained by uncertainty in the measurements.

Fig. 6 shows diffuse fraction as a function of air mass for one clear day in September for all eight ISIS stations. Figs. 4 and 5 support the claims that short-term diffuse fraction is dependent on factors other than clearness index. Again, drier locations, such as Albuquerque and Salt Lake City, appear to be less affected by air mass than locations like Seattle that have higher relative humidity.

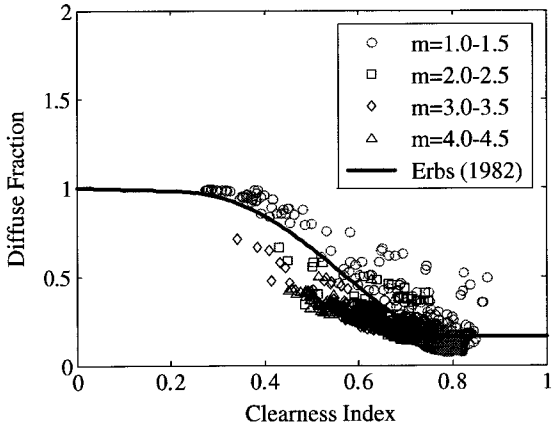

Fig. 4. The dependence of diffuse fraction on air mass for June 2002, Hanford, CA.

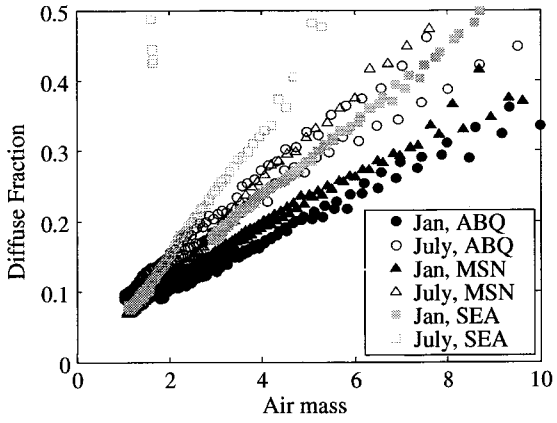

Fig. 5. Diffuse fraction as a function of air mass for clear January and July days in Seattle, Albuquerque, and Madison.

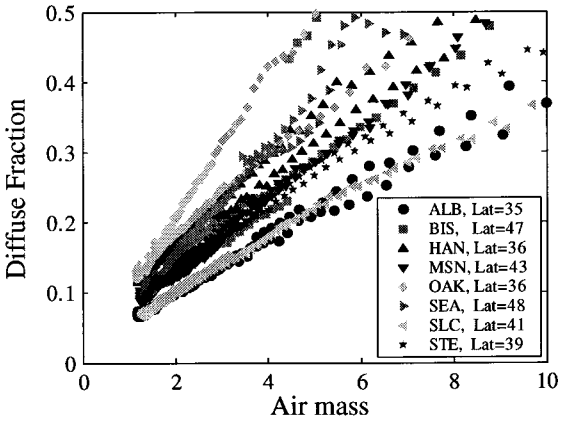

Fig. 6. Diffuse fraction as a function of air mass for clear September days in eight ISIS stations.

2.2. Frequency distribution of solar radiation

The frequency distribution, i.e., the relative number of cloudy, average and sunny time periods that together form the average, is important in determining the performance of solar energy systems. The distribution can be represented in a non-dimensional manner in terms of the fractional time of occurrence of the daily clearness index, K_T, the ratio of the total radiation to the extraterrestrial radiation for a particular day. Liu and Jordan (1960) showed that cumulative distributions representing the long-term average distribution of daily clearness index values are a unique function of $\overline{K}_T$, the monthly daily average clearness index. Generalized distribution curves were developed by Liu and Jordan, and equations representing these curves were developed by Bendt et al. (1981), based on 20 years of data from 90 locations.

Suehrcke and McCormick (1988) showed that the frequency distribution of 1-min data in Perth, Australia, showed a distribution that significantly differed from the Bendt distributions. In a similar analysis of 1-min data in San Antonio, Albany, and Atlanta, Gansler (1993, 1995) also showed significant differences from the Bendt et al. distributions. Fig. 7 shows the cumulative frequency distribution of 3-min clearness indices for Sterling, VA, for a one year time period. Clearness indices were grouped according to their hourly clearness index for comparison to the Bendt et al. regression.

Suehrcke noted that, at short time intervals, the solar energy takes on an "on–off" behavior depending on whether the sun is obscured by clouds at the time of the measurement. This "on–off" behavior was not observed in the eight locations used in this study; however the distributions did significantly differ from those reported by Bendt et al. Although the Bendt regressions were developed for daily clearness indices, it had been shown previously by Whillier (1953) that the frequency distributions of hourly clearness indices in a day were a unique function of the daily clearness index, similar to the daily clearness indices being a unique function of the monthly average daily clearness index. Fig. 7 shows that that the distributions based on daily and hourly data do not well represent the distributions prepared using 3-min data.

The air mass dependence of the short-term distribution of solar radiation was investigated. Fig. 8 shows the frequency distribution of 3-min clearness indices for Albuquerque, grouped by hourly clearness index and by air mass. The strong air mass dependence, particularly at high air mass values, was observed in all eight locations and supports Gansler's conclusion that frequency distribution regressions for short-term radiation data should be developed as functions of air mass and

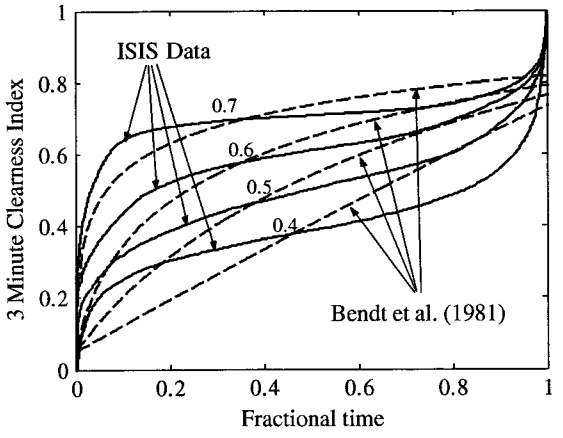

Fig. 7. Frequency distribution of 3-min clearness indices in Sterling, VA, grouped by hourly average.

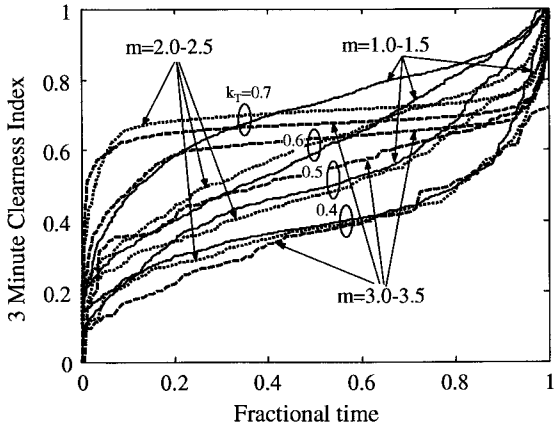

Fig. 8. Frequency distribution of 3-min clearness indices in Albuquerque, NM, grouped by air mass, m and hourly average.

hourly clearness index. The development of such regressions would allow locations, where short-term data is unavailable, to use available hourly averages to predict the distribution of short-term clearness indices. If a diffuse fraction regression were also developed for short-term data, the diffuse and beam components of the total radiation could also be estimated. If it were not computationally prohibitive, these short-term data could then be used in calculations and performance analyses. Attempts at such regressions have been made by Gansler (1993), Skartveit and Olseth (1992) and Tovar et al. (1998). The meteorological data (i.e., ambient temperature, relative humidity, turbidity) needed to develop short-term diffuse fraction regressions and frequency distribution curves are not measured at the ISIS stations.

3. Radiation on a tilted surface

Calculation of the hourly radiation on a tilted surface, I_T, allows for a quantitative estimate of the impact of using short-term data rather than hourly data. Radiation data on a tilted surface were calculated using the Perez regression (Perez et al., 1990) in three different ways for short-term data and hourly data.

The first method, denoted "Gbn, Gd", uses the beam normal and diffuse components of solar radiation from the data set to calculate the other components (i.e., the beam horizontal radiation is obtained by projection of the beam normal radiation, and the global horizontal radiation is the sum of beam and diffuse horizontal. The second method, denoted "G, Gd", uses the global horizontal and diffuse horizontal radiation from the data set. The beam horizontal is obtained by subtraction and projected to recalculate the beam normal radiation.

The third method, denoted "Erbs", applies the Erbs et al. (1982) hourly diffuse fraction regression to the global horizontal radiation data to calculate the diffuse horizontal radiation and then proceed as in second method. In all cases, the tilted surface radiation is calculated from the beam and diffuse component using Perez et al. (1990) regression. It is also possible to calculate the required radiation components from the global horizontal and the beam normal radiation, but this combination has been found to give results very similar to those obtained using second method and its results are not presented.

The three methods used to calculate radiation components and tilted surface radiation are applied directly to short-term data and to hourly data that was obtained by summing the short-term values. The tilted radiation (short-term or hourly) is then summed to calculate the monthly average daily irradiation on a tilted surface. Table 2 presents the results obtained for Madison, WI using 1-min and hourly data.

For short-term (1-min) data, the results obtained with the three methods of calculating radiation components are within 3% of each other, but there is a trend that both the "G, Gd" and Erbs correlation yield lower tilted radiation values than the "Gbn, Gd" method in winter and higher values in summer. Both methods use the measured global horizontal radiation, which is known to be slightly underestimated due to re-radiation from the PSP to the sky (that can be as large as 30 W/m^2) and to the cosine error (underestimated values at high incidence angle). The fact that tilted radiation is mostly underestimated in winter can be attributed to three different causes: higher cosine error on the global horizontal measurements, higher infrared cooling of the instrument in more frequent clear sky conditions, and higher relative importance of similar offset errors given the lower radiation levels. On the other hand, during clear summer days the beam radiation calculated from the measured global and diffuse radiation values is very often higher than the projected value of the beam normal radiation recorded by the normal incidence pyrheliometer. The Erbs regression does not have a significant impact on the tilted radiation values when compared to the ("G, Gd") method, which also uses the measured global horizontal radiation.

The use of hourly data instead of 1-min data does not have a significant impact on monthly average daily tilted radiation values in the selected data set for Madison, WI. All results using hourly data are within 1% of their corresponding results using 1-min data, except for some winter months where the difference is 2% when the Erbs regression is used to estimate diffuse radiation.

Table 3 presents the results obtained for Seattle, WA using 3-min and hourly results. The different methods to calculate the radiation components and tilted surface for Seattle produce results similar to those observed for Madison, but the trends are stronger. The use of measured global horizontal radiation leads to underestimates of the tilted radiation by about 10% in winter months, compared with the method which uses beam normal and diffuse horizontal radiation. In summer, tilted radiation is overestimated by less than 3%. The use of Erbs regression to calculate diffuse radiation reinforces these trends, with differences up to −20% in winter and +5% in summer. Here again, the use of hourly values instead of short-term data does not change the results by more than 1% except for the third method in which the Erbs regression is applied in winter months. In this case, the use of smoother hourly-averaged data results in a larger underestimate of tilted radiation compared with the first method in which actual diffuse data are used.

A conclusion from this study is that the monthly average radiation on a tilted surface is not significantly different when calculated from hourly or short-term horizontal data despite the observed short-term variability in the diffuse fraction and its dependence on the air mass and moisture level. The effects of this variability

Table 2
Monthly-average daily radiation (MJ/m^2) on a surface tilted at the latitude angle for Madison, WI

	1-min Data			1-h Data		
	Gbn, Gd	G, Gd	Erbs	Gbn, Gd	G, Gd	Erbs
January	12.9	12.7	12.8	12.9	12.5	12.7
February	17.1	16.9	17.0	17.1	17.0	17.0
March	16.2	16.2	16.2	16.2	16.2	16.2
April	17.4	17.6	17.5	17.4	17.6	17.5
May	18.2	18.6	18.5	18.1	18.6	18.5
June	19.0	19.4	19.3	19.1	19.4	19.3
July	19.4	20.1	19.9	19.3	20.0	19.8
August	20.8	21.4	21.2	20.7	21.2	21.1
September	18.5	18.8	18.7	18.5	18.8	18.7
October	12.7	12.5	12.5	12.7	12.5	12.5
November	11.3	11.1	11.1	11.3	11.1	11.2
December	11.3	11.1	11.2	11.3	11.1	11.2

Table 3
Monthly-average daily radiation (MJ/m^2) on a surface tilted at the latitude angle for Seattle, WA

	3-min Data			1-h Data		
	Gbn, Gd	G, Gd	Erbs	Gbn, Gd	G, Gd	Erbs
January	6.9	6.2	6.4	7.0	6.1	6.4
February	8.7	8.2	8.3	8.8	8.2	8.3
March	12.1	11.9	11.9	12.1	11.8	11.9
April	13.5	13.6	13.5	13.6	13.7	13.6
May	17.5	17.8	17.7	17.6	17.9	17.7
June	18.1	18.5	18.3	18.0	18.4	18.3
July	20.1	20.5	20.2	20.1	20.5	20.3
August	22.0	22.2	22.0	22.0	22.2	22.1
September	18.3	18.0	18.0	18.3	18.0	18.0
October	10.1	9.6	9.7	10.2	9.6	9.8
November	8.1	7.4	7.6	8.2	7.4	7.6
December	3.9	3.5	3.6	3.9	3.4	3.6

apparently cancel when calculations are integrated over monthly periods. On a hourly basis, differences up to 30 W/m^2 were noticed between the value calculated by applying the Perez regression to hourly data instead of using minute data and summing 1-min tilted radiation values. The standard deviation of the difference over the selected months is about 5 W/m^2. The next section will show that the sub-hourly variations play a more important role in solar radiation utilizability.

The same tilted radiation values were calculated using the method proposed by Liu and Jordan (1962), which does not consider the anisotropic behavior of diffuse radiation in the calculation of radiation on a tilted surface. Results show close agreement between the monthly-average daily radiation calculated by integration of hourly and short-term data using the same radiation model.

4. Utilizability

Utilizability is defined as the fraction of the solar radiation incident on a surface that exceeds a specified threshold or critical level, I_C. The utilizability concept can be used to evaluate the performance of many types of solar energy systems, including active, passive and photovoltaic systems (Klein and Beckman, 1984). Monthly average daily utilizability is the fraction of the total solar radiation incident on a surface during a month that exceeds the critical level. The monthly average daily utilizability, $\overline{\phi}$, has been calculated assuming the critical level is constant. Using hourly data, the monthly-average daily utilizability can be calculated using Eq. (2). With short-term data, an additional summation is needed for the minutes within the hour.

$$\overline{\phi} = \frac{\sum_{\text{days}} \sum_{\text{hours}} (I - I_C)^+}{\sum_{\text{days}} \sum_{\text{hours}} I} \tag{2}$$

Utilizability was determined for a range of critical levels by applying critical levels to short-term and hourly beam normal radiation values. Short-term beam normal utilizability was calculated from both measurements of beam normal and from the difference between measured global and diffuse radiation. In this latter case, both diffuse radiation measurements and the Erbs regression were used to determine the diffuse fraction. Utilizability analyses for these short-term beam normal data were compared to the ISIS 3-min beam normal data, as shown in Fig. 9.

Plots a and b in Fig. 9 show the discrepancy between using actual measurements of beam normal and using values calculated from other available data for January in Seattle. This difference results from the measurements having been taken with independent instruments. The magnitude of this difference varies by location, and

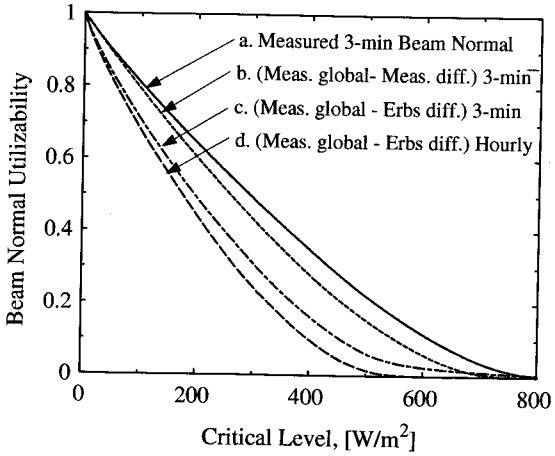

Fig. 9. Comparison of average daily beam normal utilizability for January in Seattle using four different ways of obtaining the beam normal radiation.

months where the total minus diffuse data resulted in greater utilizability were also observed.

Currently, performance analyses in locations where limited data are available use hourly diffuse fraction regressions to determine diffuse and beam radiation from the available total. Comparison of the results in Fig. 9 (plots a and c) shows that such analyses can greatly underestimate the true performance of a system. Applying the Erbs diffuse regression to 3-min data for this month and location significantly underestimates utilizability.

Plot d in Fig. 9 is obtained by applying the Erbs regression to hourly data, as is more commonly done. This option also usually resulted in an underestimate of utilizability but there were months and locations where the Erbs regression resulted in an overestimate of the utilizability. This result occurs because the Erbs regression can both underestimate and overestimate the amount of beam radiation, depending on the type of day, as seen in Fig. 2. The distribution of days, therefore, greatly influences the results of the utilizability analyses.

The argument for using short-term radiation data rather than hourly data is apparent in Fig. 10, where utilizability curves versus the critical level are compared for five different time steps for Madison, WI in July. Variations in beam normal radiation during an hour can lead to greater utilizability than would be indicated in an analysis using hourly data. The utilizability for beam radiation based on hourly data is lower than that based on short-term data because of the increased variability is evident in the short-term data. For the same total radiation, utilizability is higher when solar radiation is more variable, as first noted by Whillier (1953). This result was found consistently among all months and all locations, although the magnitude of the underestimation varied. The inset in Fig. 10 shows how the data time step affects the utilizability for a given critical level. The results show that half of the variability that is present in 1-min data is already lost if a 15-min time step is used.

Fig. 11 shows beam normal utilizability curves obtained for different months at different locations, for short-term and hourly data. Differences between utilizability values calculated with short-term and 1-h data are usually less than 0.1 for all critical levels. Maximum differences often occur at a critical level between 200 and 400 W/m^2 and represent 10–30% of the utilizability obtained with short-term data (higher differences are obtained for months and locations with a lower monthly

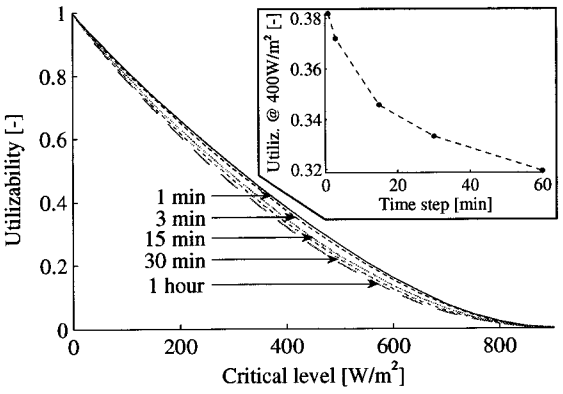

Fig. 10. Comparison of average daily beam normal utilizability for July in Madison, WI for different data time steps. Inset: utilizability at a critical level of 400 W/m^2 versus data time step.

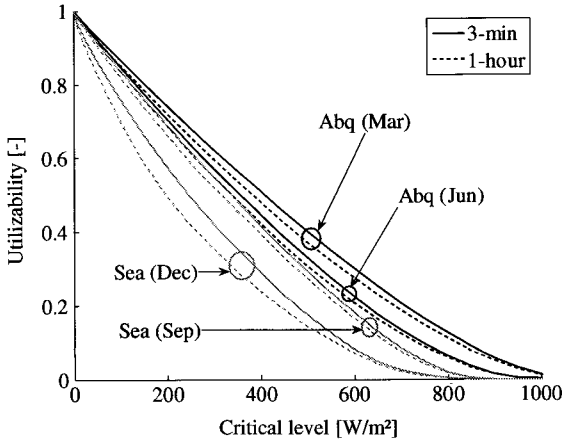

Fig. 11. Average daily beam normal utilizability for different months at different locations: comparison between 3-min data and hourly data.

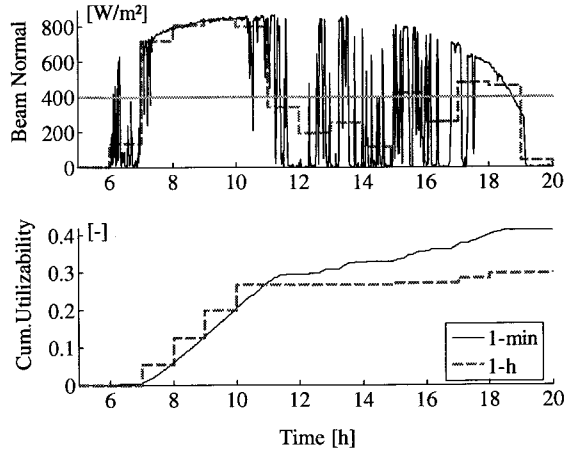

Fig. 12. Beam normal radiation and integrated utilizability for July 5 in Madison, using hourly and 1-min data (critical level = 400 W/m^2).

utilizability). In extreme cases, differences of 50% were noted between the daily average monthly utilizability values calculated from the 3-min and from the hourly data.

Fig. 12 illustrates the importance of radiation variability on calculated utilizability in a more graphical way: the upper part of the plot is the measured beam normal radiation on July 5 in Madison, WI (1-min and hourly values). The horizontal line at 400 W/m^2 represents a critical level for utilizability. The lower part of the plot shows the integrated utilizability versus the time of the day, both for 1-min and hourly data. While the hourly integration has virtually no impact during clear hours (beginning of the day), values obtained in the presence of scattered clouds (afternoon) are very different and lead to a difference in the daily utilizability of 30% for that day.

5. Conclusions

The analyses presented here confirm that the variations in solar radiation within an hour cannot be considered negligible when conducting performance analyses of solar energy systems. Although the monthly average radiation calculated using hourly data is quite close to the result obtained using short-term data, the utilizability can be significantly different. The distribution of short-term radiation within an hour results in greater utilizability, if the short-term data varies significantly. On a clear day when the variation within the hour is minimal, the magnitude of the difference decreases. On a partly cloudy day when large variations exist within the hour, hourly analyses will consistently underestimate the true performance of a system. As seen in Fig. 11, monthly average beam normal utilizability can be underestimated by 10–30% for critical levels between 200 and 500 W/m^2. Depending on the critical level, location, and month, utilizability analyses using hourly data rather than short-term data can underestimate performance anywhere between 5% and 50%. Further work will assess the importance of short-term variations in solar radiation when simulating the performance of solar energy conversion systems using the hourly data that are typically available.

Acknowledgments

The support of National Science Foundation for G. Vijayakumar is gratefully acknowledged. The authors also wish to thank John A. Augustine, Christopher R. Cornwall and Gary Hodges and the ISIS program for making the high quality data freely available and providing help in interpreting these data.

References

Bendt, P., Collares-Pereira, M., Rabl, A., 1981. The frequency distribution of daily insolation values. Solar Energy 27, 1–5.

Duffie, J.A., Beckman, W.A., 1991. Solar Engineering of Thermal Processes, second ed. Wiley Interscience, New York, ISBN 0-471-51056-4.

Dutton, E.G., Michalsky, J.J., Stoffel, T., Forgan, B.W., Hickey, J., Nelson, D.W., Alberta, T.L., Reda, I., 2001. Measurement of broadband diffuse solar irradiance using current commercial instrumentation with a correction for thermal offset errors. J. Atmos. Ocean Tech. 18, 297–314.

Erbs, D.G., Klein, S.A., Duffie, J.A., 1982. Estimation of the diffuse radiation fraction for hourly, daily, and monthly-average global radiation. Solar Energy 28, 293–302.

Gansler, R., 1993. Assessment of generated meteorological data for use in solar energy simulations. M.S. Thesis, Mechanical Engineering Department, University of Wisconsin—Madison, Madison.

Gansler, R., Klein, S.A., Beckman, W.A., 1995. Investigation of minute solar radiation data. Solar Energy 55, 21–27.

Gulbrandsen, A., 1978. On the use of pyranometers in the study of spectral solar radiation and atmospheric aerosols. J. Appl. Meteor. 17, 899–904.

Iqbal, M., 1983. An Introduction to Solar Radiation. Academic Press, New York, pp. 112–145.

Integrated Surface Irradiance Study (ISIS) Network, 2004. Available from: <http://www.srrb.noaa.gov/isis/index.html>.

Klein, S.A., Beckman, W.A., 1984. Review of solar radiation utilizability. J. Solar Energy Eng. 106, 393–402.

Liu, B.Y.H., Jordan, R.C., 1960. The interrelationship and characteristic distribution of direct, diffuse and total solar radiation. Solar Energy 4, 1–19.

Liu, B.Y.H., Jordan, R.C., 1962. Daily insolation on surfaces tilted toward the equator. ASHRAE J. 3, 53–59.

McArthur, L.J.B., 1998. Baseline Surface Radiation Network (BSRN) operations manual. WMO/TD-879, World Climate Research Program, 69p.

National Solar Radiation Data Base, 1992. Last accessed 3/9/03. Available from: <http://rredc.nrel.gov/solar/pubs/NSRDB/>.

Perez, R., Stewart, R., Seals, R., Guertin, T., 1988. A new simplified version of the Perez diffuse irradiance model for tilted surfaces. Solar Energy 39, 221–229.

Perez, R., Ineichen, P., Seals, R., Michalsky, J., Stewart, R., 1990. Modeling daylight availability and irradiance components from direct and global irradiance. Solar Energy 44 (5), 271–289.

Perez, R., Ineichen, P., Maxwell, E., Seals, R., Zelenka, A., 1992. Dynamic global to direct irradiance conversion models. ASHRAE Trans. 98 (Pt. 1), 354–359.

Reindl, D.T., Beckman, W.A., Duffie, J.A., 1990. Diffuse fraction correlations. Solar Energy 45 (1), 1–7.

Saluja, G.S., Muneer, T., 1986. Letter to the Editor commenting on "A new look at the correlation of *kd* and *kt* ratios and at global solar radiation tilt models using one-minute measurements". Solar Energy 36 (2), 197.

Skartveit, A., Olseth, J.A., 1992. The probability density and autocorrelation of short-term global and beam irradiance. Solar Energy 49, 477–487.

estimation of radiation on a tilted surface also requires knowledge of the beam and diffuse components. If only total radiation is known, the diffuse and beam components can be estimated using diffuse fraction regressions.

Fig. 2 is a plot of the measured diffuse fraction as a function of clearness index based on 3-min data in Madison, WI for December 2002. (Note that data points very close to sunrise/set have been removed when the measured diffuse radiation is lower than 15 W/m^2.) This plot is typical of the diffuse fraction plots observed for other months and locations. In Fig. 2(a), the diffuse fractions were determined by dividing the measured diffuse horizontal irradiance by the measured global horizontal irradiance. This method is denoted "G, Gd" in the following discussion. Values larger than 1 are mainly caused by an erroneous offset that affects Solid Black Detector Precision Spectral Pyranometers (PSP), which are used to measure global radiation in the ISIS network. The offset can be attributed to infrared cooling of the glass hemispheres, which in turn cools the detector and causes a negative offset in the response produced by this instrument (Gulbrandsen, 1978). Correction methods have been developed for diffuse radiation measurements (Dutton et al., 2001) but they are not directly applicable to global radiation measurements. PSP's measuring global radiation are also affected by errors in the directional response, which can also lead to underestimated measurements.

Fig. 2(b) shows data for the same month as Fig. 2(a) using diffuse fractions calculated with the measured diffuse horizontal radiation and the measured beam normal radiation. This procedure is recommended by the World Climate Research Program's Baseline Surface Radiation Network (McArthur, 1998; cited in Dutton et al., 2001). It is denoted "Gbn, Gd" in the following discussion. The global horizontal radiation is determined by summing the calculated beam radiation on the horizontal surface (which is the product of the beam normal radiation and the cosine of the zenith angle) and the measured diffuse radiation. Diffuse fractions calculated in this manner are always between 0 and 1.

A third method of determining the diffuse irradiance from the available data is to use the measured direct beam normal to calculate the beam radiation on a horizontal surface and subtract the beam component from the measured horizontal irradiance. The effect of using diffuse radiation in these three ways on the calculated radiation for tilted surfaces is presented in the next section.

Fig. 2 also shows the diffuse fraction regression proposed by Erbs et al. (1982) based on hourly radiation measurements. Other diffuse fraction regressions are available, e.g., Reindl et al. (1990), Perez et al. (1988, 1992). However, Fig. 2 shows that any diffuse fraction model that is based solely on the clearness index will be subject to a significant scatter as other variables affect the short-term diffuse fraction. The scatter in the diffuse fraction regression equation becomes smaller for longer time periods, as noted by Saluja and Muneer (1986).

Fig. 3 shows the relationship of diffuse fraction to clearness index using for a single clear day in April in Oak Ridge, representative of clear days in other locations. The diffuse fraction regression developed by Erbs et al. (1982) is also shown. Fig. 3 indicates that, for a clear day, the diffuse radiation is overestimated when applying Erbs' regression for hourly data to the 3-min data. Note that all of the data points in Fig. 3 correspond to clear sky conditions. The variation in clearness index in this case is due to the change in air mass with time of day. This same behavior was observed for 1-min clear sky data in Madison, WI.

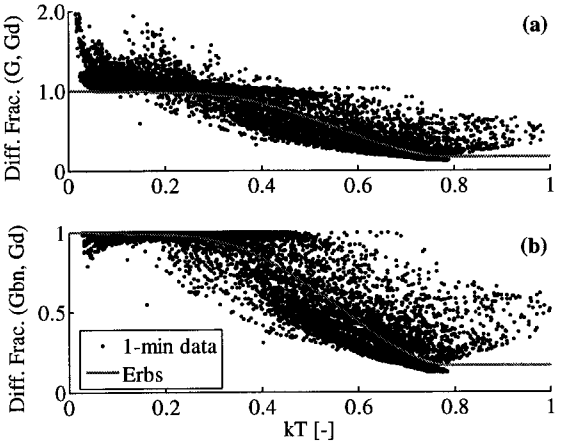

Fig. 2. 1-min Diffuse fraction as a function of clearness index for December 2002, in Madison, WI.

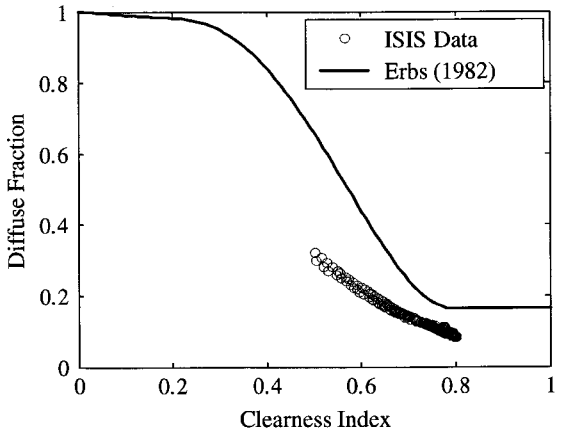

Fig. 3. Diffuse fraction as a function of clearness index for a clear April day in Oak Ridge, TN.